Control of a continuous variable transmission

Control of a Continuous Variable Transmission

WFW 94.126

Ingmar Ploemen
id. nr. 319768
September 30, 1994

coach: dr. ir. F.E. Veldpaus

Contents

1 Description of the CVT and the control problem **3**
- 1.1 Function and layout . . . 3
- 1.2 The hydraulic system . . . 3
- 1.3 Definitions . . . 4
- 1.4 CVT control in vehicles . . . 5
  - 1.4.1 General situation . . . 5
  - 1.4.2 The actual control problem . . . 5

2 CVT modelling **6**
- 2.1 Mathematical modelling of the CVT . . . 6
- 2.2 CVT response modelling . . . 7
  - 2.2.1 Simplification of the response model . . . 8

3 Design of the control law **10**
- 3.1 Pressure control . . . 10
  - 3.1.1 Rewriting the model . . . 10
  - 3.1.2 Controller design . . . 11
- 3.2 Rate of ratio control . . . 12
  - 3.2.1 Description of the existing control law . . . 12
  - 3.2.2 Rewriting the rate of ratio control law . . . 13
  - 3.2.3 Supplementary consideration . . . 14

4 Computer simulation and experiments **15**
- 4.1 Development of the pressure model . . . 15
- 4.2 Simulating the whole CVT behaviour in SIMULINK . . . 18
  - 4.2.1 The CVT model block . . . 18
  - 4.2.2 The pressure control and rate of ratio change control blocks . . . 19
- 4.3 Experiments . . . 20
- 4.4 Results . . . 20

5 Conclusions and recommendations **23**
- 5.1 Conclusions . . . 23
- 5.2 Recommendations . . . 23

A Simulink block schemes **25**

B Matlab program for fitting transferfunctions **30**

C Simulink block scheme for generating noise signals **32**

D Initialisation of all variables **33**

Chapter 1

Description of the CVT and the control problem

1.1 Function and layout

The Continuous Variable Transmission (CVT) in a hybrid drive line has two main functions. The first is to transmit a torque from the input shaft to the output shaft, allowing these shafts to rotate with different and varying speeds. The second is to either accelerate or decelerate the vehicle and the flywheel by means of varying the CVT ratio.

In this hybrid drive line a transmatic type CVT is used. This CVT consists of a metal belt composed of thin V-elements and strings, mounted between two V-shaped, adjustable pulleys. The CVT pulleys in the hybrid transmission have equal piston areas, and hence, the CVT is symmetrical.
One of the conical sheaves of each pulley can move in axial direction. By means of an oil pressure in a hydraulic chamber the belt is clamped between the sheaves of each pulley. The resulting tensile force in the strings, combined with a pushing force between the V-elements, allows the CVT to transmit a torque. Shifting of the sheaves in axial directions varies the running radius of the belt and, hence, varies the transmission ratio.

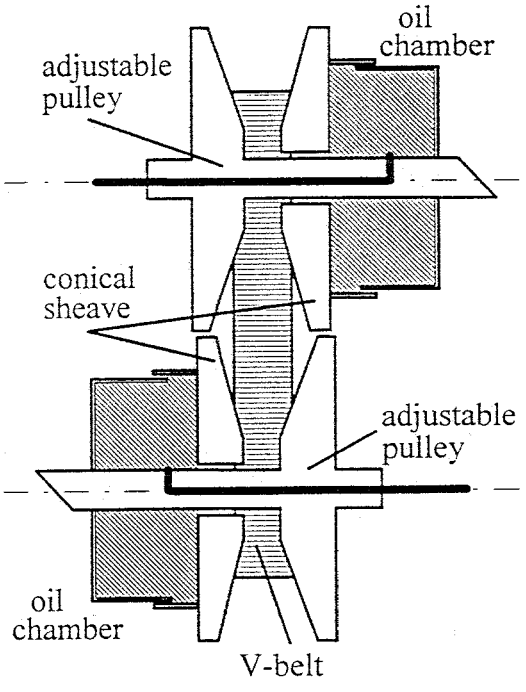

Figure 1.1: CVT schematic layout

1.2 The hydraulic system

The hydraulic system incorporates a servo valve and a high pressure circuit, which provides the operating pressure for the CVT. In this system an accumulator assures a nearly constant

line pressure, independent of the flow requirements of the valves. This constant line pressure has been set at 70 bar.

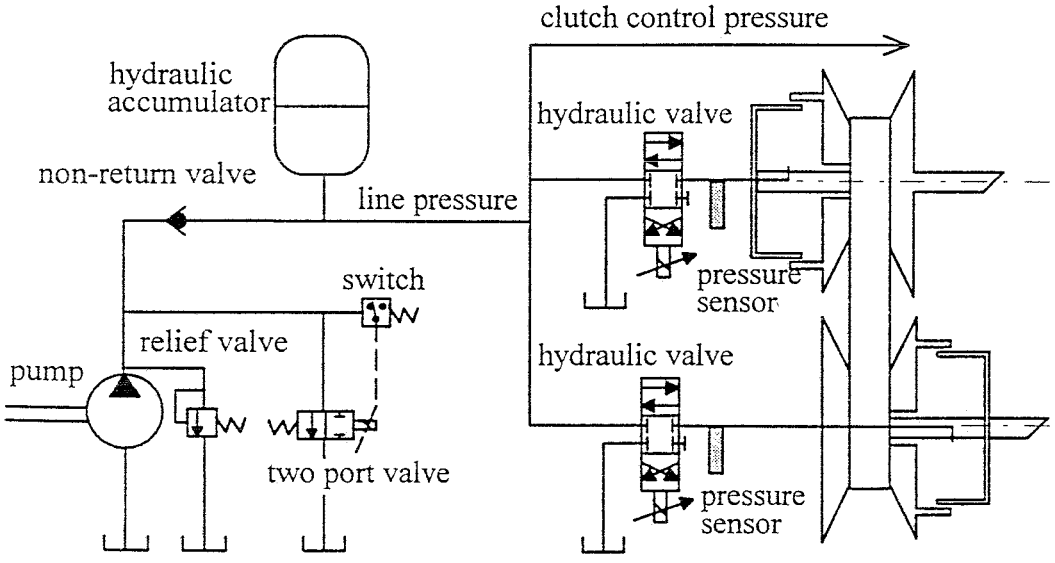

Figure 1.2: Main components of the hydraulic circuit for the CVT in the hybrid drive line

The electro-hydraulic servo valve contains an electrically activated pilot stage and a hydraulically activated main valve. The position of the main valve is measured and a correction signal to the pilot valve results in an adjustment of the position of the main valve. The valve requires only a small electrical signal, it uses hydraulic power to control the main valve. Therefore, a minimum pressure is required to operate this type of valve. The relation between the flow Q through the valve and the voltage u applied to the pilot stage is:

$$Q = V(u, \Delta p) \tag{1.1}$$

where Δp is the pressure drop over the valve.

In the existing control system the valve electronics were modified in order to optimize the valves for pressure control. In this report the original valve characteristics are used, because the valves are used for pressure and flow control simultaneously.

1.3 Definitions

In conventionally powered vehicles, the primary CVT pulley is defined as the pulley which is driven by the engine. The secondary pulley is defined as the pulley at the output shaft of the transmission. In the hybrid drive line the same definition is used.

The inputs of the system are the voltages u_p and u_s of the hydraulic valves, where the lower indices s and p refer to the secondary, and the primary pulley, respectively. The outputs are the pressures in the pulley chambers: p_p and p_s, and the angular velocities ω_p and ω_s of the pulleys.

The CVT ratio i follows from the relation $\omega_s = i\,\omega_p$. The time derivative of this ratio is called the *rate of ratio change.*

1.4 CVT control in vehicles

1.4.1 General situation

For vehicles, equipped with a CVT, various control objectives can be identified:

- controlling the CVT rate of ratio change. This allows the inertias to be accelerated or decelerated. This type of control is essential for the hybrid vehicle and will be discussed in this report.
- keeping the CVT ratio at one specific operating point i.e., a single constant ratio. In the hybrid drive line this is used during mode shifts when clutches have to be synchronised. This type of control won't be discussed in this report.
- shifting the CVT ratio from one operating point to another ("point-to-point" control). This is used during normal driving in a conventional vehicle, when the output power is controlled by varying the engine speed. In this case the specific trajectory, by which the new ratio is reached is relevant for the driveability of the vehicle. This type of control is also sometimes used in the hybrid vehicle, but won't be discussed in this report

1.4.2 The actual control problem

In the hybrid drive line, large torques are transmitted, from flywheel to vehicle and vice versa. In order to maintain a sufficiently large clamping force to prevent belt slip under all circumstances, pressure control is used on the secondary (driven) pulley. In order to control the rate of ratio change, an oil flow is directed into the primary (driving) pulley. So the control problem is to realize a certain pressure p_s in the secondary pulley chamber and a certain change ρ of the rate of ratio, where $\rho = di/dt$.

If the CVT can realize the desired rate of ratio change within a very short time, the drive line and the CVT can be controlled independently. So the goal is to realize a control system for the CVT with a sufficiently high closed loop bandwidth.

Chapter 2

CVT modelling

2.1 Mathematical modelling of the CVT

In this report the CVT modelling as given by E. Spijker (1994) is used. Only the essential equations for the control problem will be mentioned.

- The relation between the required oil flow to the hydraulic cylinder of a pulley and the rate of ratio change:

$$Q_k = f_k \frac{di}{dt}; \quad k = p, s \tag{2.1}$$

where f_k is a nonlinear function of the CVT ratio i. A graphical representation of this function $f_k = f_k(i)$ is given in Figure 2.1.

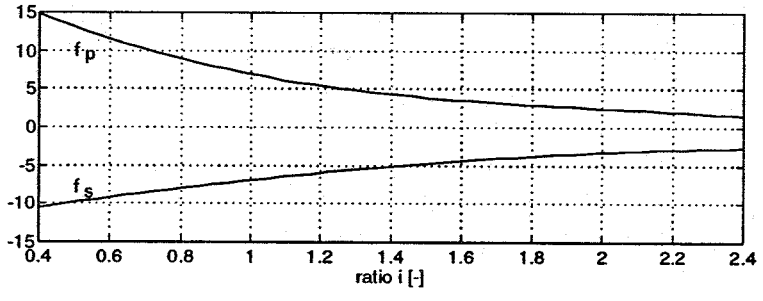

Figure 2.1: The function $f_{p,s}$ for the primary, respectively the secondary pulley

- The relation between the output torque and the rate of ratio change:

$$T_{out} = \omega_{flw} \left(\frac{i^2}{\eta J_{flw}} + \frac{1}{J_{veh}} \right) \frac{di}{dt} \tag{2.2}$$

where J_{flw} and J_{veh} are the moment of inertia of the flywheel respectively the equivalent moment of inertia of the vehicle.

- The minimum pressure in the secondary pulley chamber necessary to prevent belt slip for a given torque T:

$$p_{s,min} = \frac{cos\beta\, T_s}{2\,\mu\, A\, r_s} \tag{2.3}$$

where β is the top angle of a pulley sheave, μ is the Coulomb friction coefficient and r_s is the radius of the belt on the secondary pulley sheave. Since a safety margin is used in practice, the expression becomes:

$$p_s = c_{safe}\frac{cos\beta\, T_s}{2\,\mu\, A\, r_s} \tag{2.4}$$

For CVT pressure control a safety margin of $c_{safe} = 1.3$ is normally used.

Another essential equation is the valve characteristic in Eq.1.1. This relation between the oil flow Q [l/s] and the voltage u_p [V] is described in the manual of the valves:

$$Q = c_{valve}\, u\sqrt{\Delta p} \tag{2.5}$$

where Δp [bar] is the pressure drop over the valve. This pressure drop equals the difference between the line pressure p_{line} and the pressure in the pulley chamber p_s.

2.2 CVT response modelling

The CVT response depends very much on the operating conditions, like the ratio i and the oil temperatures. That would cause a lot of problems when developing an analytical model of the CVT. Besides that, the CVT is highly non-linear and this would result in a very complicated model. Therefore no further attention will be paid to the analytic modelling of the CVT and its dynamic response. The relation between the inputs u_p and u_s and the outputs p_p and p_s of the CVT will be derived on the basis of experiments performed on the CVT.

By means of these experiments the transfer functions can be obtained and the following linear model for the pressure response holds:

$$\begin{bmatrix} p_p(s) \\ p_s(s) \end{bmatrix} = \begin{bmatrix} H_{pp}(s) & H_{ps}(s) \\ H_{sp}(s) & H_{ss}(s) \end{bmatrix} \begin{bmatrix} u_p(s) \\ u_s(s) \end{bmatrix} \tag{2.6}$$

As a simplification only experiments at ratio $i = 1$ are performed, because the CVT is symmetric for that ratio. In Spijker (1994) in this way the transfer functions $H_1(s) = \frac{p_p(s)}{u_p(s)}$ and $H_2(s) = \frac{p_s(s)}{u_p(s)}$ were obtained by applying a white noise signal u_p to the primary valve (see Fig. 2.2). Because of the symmetrical CVT, the transfer functions from secondary valve u_s to the pressures p_p and p_s are also known and the following relations hold: $H_{ss}(s) = H_{pp}(s) = H_1(s)$ and $H_{ps}(s) = H_{sp}(s) = H_2(s)$. This results in the following linear "black box" model for the CVT response, valid only for $i = 1$:

$$\begin{bmatrix} p_p(s) \\ p_s(s) \end{bmatrix} = \begin{bmatrix} H_1(s) & H_2(s) \\ H_2(s) & H_1(s) \end{bmatrix} \begin{bmatrix} u_p(s) \\ u_s(s) \end{bmatrix} \tag{2.7}$$

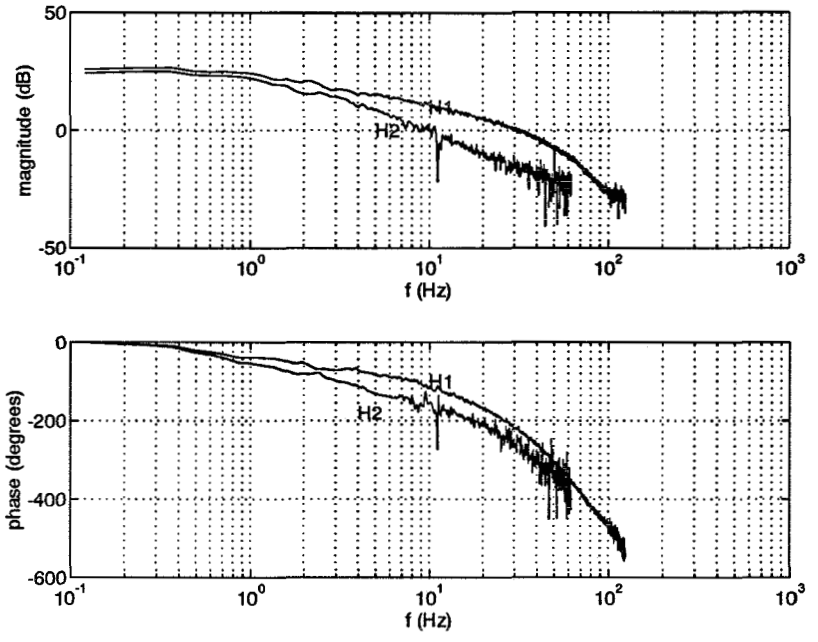

Figure 2.2: Bode plots of the transfer functions H_1 and H_2

2.2.1 Simplification of the response model

Because the transfer functions approximately have a first order character as can be seen in Fig. 2.2, the measured transfer functions H_1 and H_2 are fitted with a first order model, so:

$$H_1(s) \simeq \frac{b_1}{s+a_1}; \quad H_2(s) \simeq \frac{b_2}{s+a_2}; \tag{2.8}$$

Substitution of Eq.2.8 into Eq.2.7 gives:

$$\begin{bmatrix} p_p(s) \\ p_s(s) \end{bmatrix} = \begin{bmatrix} \frac{b_1}{s+a_1} & \frac{b_2}{s+a_2} \\ \frac{b_2}{s+a_2} & \frac{b_1}{s+a_2} \end{bmatrix} \begin{bmatrix} u_p(s) \\ u_s(s) \end{bmatrix} \tag{2.9}$$

This is still a very complicated model that is not suited for designing a control law, because not p_p and p_s have to be controlled, but p_s and ρ, where ρ is a nonlinear function of p_p. Therefore Spijker makes the assumption that there is no interaction between the pulley chambers, i.e. he says that $H_2 = 0$. This is a very rude simplification that is in conflict with the reality, but as a first attempt it was good enough to derive a working control law.

In this report an attempt is made to take into account this interaction between the pulley chambers. However a simplification is made by assuming that:

$$H_2 = \alpha H_1 \tag{2.10}$$

Looking at the shapes of H_1 and H_2 on linear axes and the value of $|H_2|/|H_1|$ in Figure 2.3 it can be seen that it is not right to assume that the constant α is independent of the frequency ω, especially not for small values of ω. The main motivation for the assumption that α is

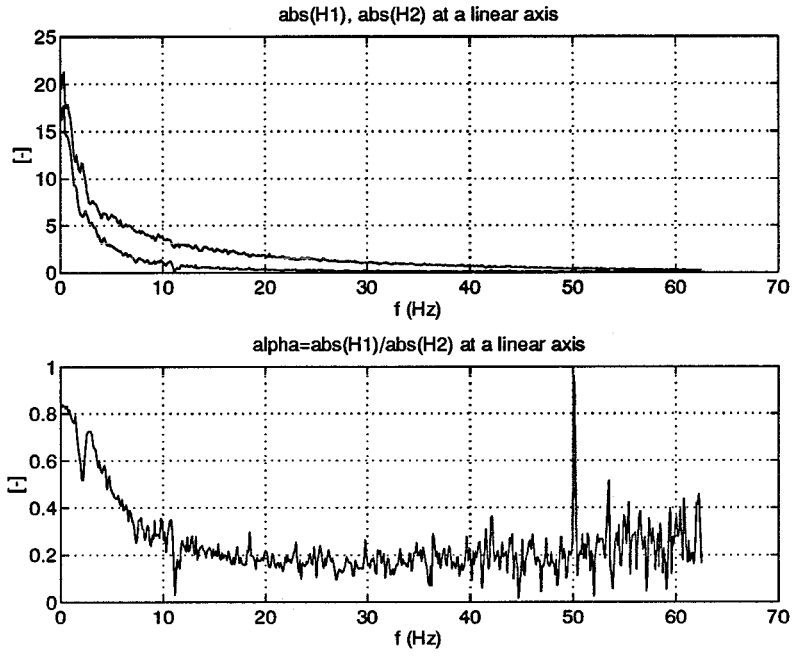

Figure 2.3: Transfer function H_1 and H_2 on a linear axis, and value of α

constant is that it results in a simple model that takes into account the interaction between the pulley chambers. From $H_2 = \alpha H_1$ it is easily seen that $a_1 = a_2 \equiv a$ and $b_2 = \alpha b_2 \equiv \alpha b$, so:

$$\begin{bmatrix} p_p(s) \\ p_s(s) \end{bmatrix} = \begin{bmatrix} \frac{b}{s+a} & \alpha \frac{b}{s+a} \\ \alpha \frac{b}{s+a} & \frac{b}{s+a} \end{bmatrix} \begin{bmatrix} u_p(s) \\ u_s(s) \end{bmatrix} \tag{2.11}$$

Converting this relation into the time domain gives:

$$\begin{bmatrix} \dot{p}_p \\ \dot{p}_s \end{bmatrix} = -a \begin{bmatrix} p_p \\ p_s \end{bmatrix} + b \begin{bmatrix} 1 & \alpha \\ \alpha & 1 \end{bmatrix} \begin{bmatrix} u_p(s) \\ u_s(s) \end{bmatrix} \tag{2.12}$$

This model can be used for designing a control algorithm. By substituting $\alpha = 0$ into 2.12 one arrives at the model Spijker used for the design of his control law.

Chapter 3

Design of the control law

Although Spijker used only a simple model for the design of a control law, he managed to realize a control algorithm, that satisfied his demands to a certain extend. The main goal of this report is to find out whether adding the interaction between the pulley chambers to his control strategy will result in a better control law. That's why in this report the same concepts are used as in Spijker (1994).

3.1 Pressure control

3.1.1 Rewriting the model

Pressure control will be used for the secondary, driven, pulley. As stated at the end of section 2.2.1 Spijker used a model of the following structure for designing the pressure control law:

$$\dot{p}_s = -a\,p_s + b\,u_s \tag{3.1}$$

In this equation p_s depends only on the input u_s. That enables Spijker to design a SISO controller for the pressure control. The second equation of model 2.12, that will be used for the controller design, shows us that p_s depends also on the input u_p:

$$\dot{p}_s = -a\,p_s + b\,u_s + b\,\alpha u_p \tag{3.2}$$

Because we want to follow the same strategy as Spijker we will have to rewrite these equations. We can rewrite the first equation of 2.12 as:

$$u_p = \frac{1}{b}(\dot{p}_p + a\,p_p - b\,\alpha\,u_s) \tag{3.3}$$

Substitution into Eq.3.2 gives:

$$\dot{p}_s = -a\,p_s + b(1-\alpha^2)\,u_s + \alpha(\dot{p}_p + a\,p_p) \tag{3.4}$$

In this equation p_s depends only on one input, which enables the design of a SISO controller. If we compare Eq.3.1 with Eq.3.4 we see that Eq.3.4 indeed takes into account the interaction between the pulley chambers. A raise of the pressure p_p will result in a rising value for the pressure p_s, which is caused by the interaction via the belt.

3.1.2 Controller design

The desired value $p_{s,set}$ follows from Eq.2.4. The proposed linear control law is:

$$u_s = -k_c\, p_s + m_c\, p_{s,set} - c_c(\dot{p}_p + a\, p_p) \tag{3.5}$$

In order to obtain the appropriate behaviour under all operating conditions the control parameters k_c, m_c and c_c are adapted on-line.
Substitution of Eq.3.5 into 3.4 gives:

$$\dot{p}_s = c_1\, p_s + c_2\, p_{s,set} + c_3\,(\dot{p}_p + a\, p_p) \tag{3.6}$$

where:

$$c_1 = -a - (1-\alpha^2) b\, k_c,\;\; c_2 = (1-\alpha^2) b\, m_c,\;\; c_3 = \alpha - (1-\alpha^2) b\, c_c \tag{3.7}$$

Because the goal is to obtain a system with a desired closed loop bandwidth, as in Spijker (1994), the desired pressure behaviour is specified by means of a reference model:

$$\dot{p}_r = -a_r\, p_r + b_r\, p_{s,set} \qquad ; a_r > 0 \quad a_r = b_r \tag{3.8}$$

with the desired pressure $p_{s,set}$ as input. If $p_{s,set}$ is constant this guarantees that the reference pressure p_r converges to the desired value of $p_{s,set}$. However if $\dot{p}_{s,set} \neq 0$ then in general $p_r \rightarrow p_{s,set}$ for $t \rightarrow \infty$ doesn't hold.

In the actual implementation of the control law the parameter a_r is chosen such that the bandwidth of the reference system equals 20 Hz, because the goal was to obtain a closed loop system with a bandwidth of 20 Hz. The problem is that the simplification made by assuming that $H_2 = \alpha\, H_1$ is quite reasonable, except for frequencies lower than 15 Hz. The difference between the reference pressure p_r and the actual pressure p_s is denoted by e_p, so:

$$e_p = p_r - p_s \tag{3.9}$$

From Eq.'s 3.6 and 3.8 it can be seen that:

$$\dot{e}_p = \dot{p}_r - \dot{p}_s = -a_r\, e_p - d_1\, p_s + d_2\, p_{s,set} - d_3\,(\dot{p}_p + a\, p_p) \tag{3.10}$$

where the coefficients d_1, d_2 and d_3 are given by:

$$d_1 = c_1 + a_r,\;\; d_2 = b_r - c_2,\;\; d_3 = c_3 \tag{3.11}$$

In order to find a suitable adaptation law for k_c, m_c and c_c, such that stability is guaranteed, the following candidate Lyapunov function V is chosen:

$$V = \frac{1}{2}{e_p}^2 + \frac{1}{2}\beta\, {d_1}^2 + \frac{1}{2}\delta\, {d_2}^2 + \frac{1}{2}\gamma\, {d_3}^2; \qquad \beta, \delta, \gamma > 0 \tag{3.12}$$

Differentiation of this relation with respect to time yields:

$$\dot{V} = e_p\, \dot{e}_p + \beta\, d_1\, \dot{d}_1 + \delta\, d_2\, \dot{d}_2 + \gamma\, d_3 \dot{d}_3 \tag{3.13}$$

and, using Eq.3.10, it is seen that

$$\begin{aligned} \dot{V} \;=\; & -a_r\, {e_p}^2 + d_1\,(\beta\, \dot{d}_1 - p_2\, e_p) + d_2\,(\delta\, \dot{d}_2 + e_p\, p_{s,set}) + \\ & + d_3\,(\gamma\, \dot{d}_3 - e_p\,(\dot{p}_p + a\, p_p) \end{aligned} \tag{3.14}$$

The condition for $e_p(t) \rightarrow 0$ for $t \rightarrow \infty$ is that $\dot{V} < 0$ for each $e_p \neq 0$. This condition is satisfied if:

$$\beta \dot{d}_1 - p_2 e_p = 0 \tag{3.15}$$

$$\delta \dot{d}_2 + e_p p_{s,set} = 0 \tag{3.16}$$

$$\gamma \dot{d}_3 - e_p (\dot{p}_p + a p_p) = 0 \tag{3.17}$$

Now the adaptation laws for the controller parameters can be found. Eq.3.15 yields:

$$\dot{d}_1 = -\frac{d}{dt}[a + (1 - \alpha^2) b k_c] \tag{3.18}$$

If the model parameters a, b and α are constant or slowly varying this results in the following adaptation law for k_c:

$$\dot{k}_c = -\frac{1}{\beta} \frac{p_2 e_p}{b(1 - \alpha^2)} \tag{3.19}$$

In the same way the adaptation law for m_c follows from Eq.3.16:

$$\dot{m}_c = \frac{1}{\delta} \frac{e_p p_{s,set}}{b(1 - \alpha^2)} \tag{3.20}$$

while Eq.3.17 results in the adaptation law for c_c:

$$\dot{c}_c = -\frac{1}{\gamma} \frac{e_p (\dot{p}_p + a p_p)}{b(1 - \alpha^2)} \tag{3.21}$$

Now with the Eq.'s 3.5 and 3.19 to 3.21 the control law for pressure control of p_s is totally known. The difference with Spijker's control law is the third term in 3.5 and the term $(1 - \alpha^2)$ in the adaptation laws.

There is one problem concerning the value of $\dot{p}_p$ in Eq.3.21. Although p_p is measured the derivative isn't known. That's why in the computer implementation of the control law $\dot{p}_p$ is obtained by numerically differentiating p_p, but in an actual implementation the measurement noise might cause some serious problems.

3.2 Rate of ratio control

3.2.1 Description of the existing control law

As stated before Spijker uses flow control for the primary pulley in order to realize a certain rate of ratio change. The flow to this pulley results in a pulley sheave velocity v_p which in turn results in a rate of ratio change. Therefore he has written the relevant equations in terms of v_p. Here a summary will be given of the derivation of the control law, described at pages 58 and 59 of Spijker (1994).

The following model is proposed for the relation between oil flow Q_p through the valve and pulley sheave velocity v_p:

$$\dot{v_p} = -a_q v_p + b_q Q_p \tag{3.22}$$

For velocity control a simple linear control law is proposed:

$$Q_p = -k_q v_p + m_q v_{p,set} \tag{3.23}$$

The parameters k_q and m_q are used to obtain the desired closed-loop bandwidth of 20 Hz. The input Q_p represents the oil flow at the proportional valve. This flow depends on the input u_p of the valve and the pressure drop Δp over the valve, see Eq.1.1.The following valve control signal u_p is used:

$$u_p = d_q V^{-1}(\Delta p, Q_p) \tag{3.24}$$

Because the effects of the nonlinear valve characteristic, the temperature dependence of the oil and the neglected oil leakage flow are not known quantitatively, an adaptive parameter d_q must guarantee accurate steering of the oil flow. It is noted that $d_q = 1$ is used in the case that $u_p = V^{-1}(\Delta p, Q_p)$ is an exact representation of the inverse valve characteristics. In order to obtain a suitable value for d_q as well as to guarantee stability of the combined feedback law and parameter adaptation, a reference model is defined. This reference model has the same structure as the velocity model in Eq.3.22 and is given by:

$$\dot{v_r} = -a_{qr}\, v_r + b_{qr}\, v_{p,set} \qquad a_{qr} > 0, \quad a_{qr} = b_{qr} \tag{3.25}$$

Here the same remark should be made as for the pressure reference model 3.8, namely that the difference between $v_{p,set}$ and v_r will only be assymptotically zero for a constant value of $v_{p,set}$. Substitution of Eq.3.23 into 3.22 gives:

$$\dot{v_p} = -(a_q + b_q\, k_q) v_p + b_q\, m_q\, v_{p,set} \tag{3.26}$$

Comparing this with the reference model gives us the following relations for the parameters k_q and m_q of the control law:

$$k_q = \frac{a_{qr} - a_q}{b_q}, \quad m_q = \frac{b_{qr}}{b_q} \tag{3.27}$$

The error e_q between desired pulley sheave velocity v_r and actual velocity v_p is:

$$e_q = v_r - v_p \tag{3.28}$$

Then with the help of a Lyapunov function the following adaptation law can be derived (see Spijker (1994)):

$$\dot{d_q} = \frac{1}{\gamma}\, e_q\, v_{s,set}\ , \qquad \gamma > 0 \tag{3.29}$$

With these relations the flow control law is completely known.

3.2.2 Rewriting the rate of ratio control law

In the simulation model that will be used the pulley sheave velocity v_p isn't directly available. In order to simplify the implementation in SIMULINK and because it seems obvious to control the rate of ratio change directly instead of controlling it via pulley sheave velocities, these relations are rewritten in terms of $\rho = \frac{di}{dt}$. According to Eq.2.1 the following geometrical relation between the pulley sheave velocity and the rate of ratio change holds:

$$v_p = \frac{1}{A} Q_p = \frac{1}{A} f_p\, \rho \tag{3.30}$$

where A is the piston area. With this we can rewrite Eq.3.23 and the reference model 3.25 as:

$$Q_p = -k_q \frac{f_p}{A} \rho + m_q \frac{f_p}{A} \rho_{set} \tag{3.31}$$

and:

$$\dot{\rho_r} = -a_r \rho_r + b_r \rho_{set} + \frac{\rho_r}{f} \dot{f_p} \tag{3.32}$$

Where $\dot{f_p}$ is related to i and ρ by:

$$\dot{f_p} = \frac{df}{dt} = \frac{df}{di}\frac{di}{dt} = \frac{df}{di}\rho \tag{3.33}$$

Therefore the relation for $\dot{\rho_r}$ becomes:

$$\dot{\rho_r} = -\left(a_r - \frac{\rho_r}{f}\frac{df}{di}\right)\rho_r + b_r \rho_{set} \tag{3.34}$$

The value of a_r is about 100 times the value of the term with $\frac{df}{di}$. Hence the last term can be neglected, which gives us the following relation for $\dot{\rho_r}$:

$$\dot{\rho_r} = -a_r \rho_r + b_r \rho_{set} \tag{3.35}$$

Now we define the rate of ratio change error e_ρ as:

$$e_\rho = \rho_r - \rho = \frac{A}{f_p} e_q \tag{3.36}$$

Which gives us the following adaptation law for d_q:

$$\dot{d_q} = \frac{1}{\gamma}\left(\frac{f_p}{A}\right)^2 e_\rho \, \rho_{set} \,, \qquad \gamma > 0 \tag{3.37}$$

3.2.3 Supplementary consideration

Looking at the problem from a different point of view the values for the control parameters k_q and m_q are considered again. Looking at Eq.3.26 we can see that, for v_p being asymptotically equal to a constant value of $v_{p,set}$, the values of the controller parameters have to satisfy the following condition:

$$\frac{b_q \, m_q}{a_q + b_q \, k_q} = 1 \tag{3.38}$$

From Eq.3.27 it follows for the already derived values of these parameters (remembering that $a_{qr} = b_{qr}$):

$$k_q = \frac{a_{qr}}{b_q} - \frac{a_q}{b_q}, \qquad m_q = \frac{b_{qr}}{b_q} = \frac{a_{qr}}{b_q} = k_q + \frac{a_q}{b_q} \tag{3.39}$$

Substitution of this result into 3.38 yields:

$$\frac{b_q \, m_q}{a_q + b_q \, k_q} = \frac{b_q \, k_q + a_q}{a_q + b_q \, k_q} = 1 \tag{3.40}$$

So with these parameters v_p should asymptotically follow $v_{p,set}$, again only for a constant value of $v_{p,set}$. In fact this is logical because these values were chosen in order to obtain the same behaviour as the reference model, that does asymptotically follow $v_{p,set}$.

Chapter 4

Computer simulation and experiments

4.1 Development of the pressure model

The main problem when simulating the CVT behaviour is that there is no good mathematical model that correctly represents this behaviour.

Spijker measured p_1 and p_2 for a white noise input u_1. With the MATLAB function **spectrum** the transfer functions H_1 and H_2 were obtained, for frequencies ranging from 0 to 120 Hz. The associated coherence functions are plotted in Figure 4.1. Here we see that for H_1 there is a nearly constant coherence between u_p and p_p for frequencies up to 90 Hz. So H_1 will be rather reliable. The coherence function for H_2 gives a worse result. The value zero for a

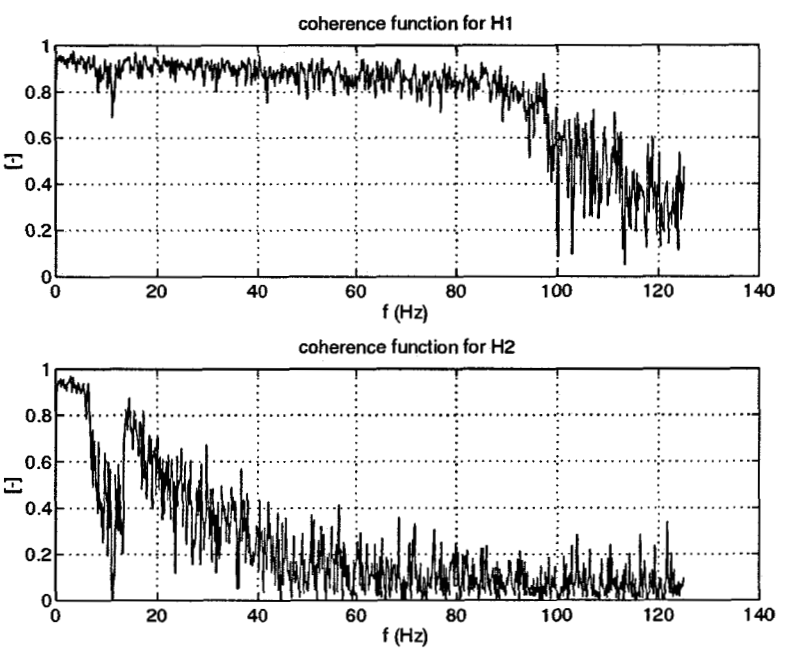

Figure 4.1: The coherence functions for H_1 and H_2

frequency of 11 Hz is caused by the rotating frequency of the pulleys of 11 Hz. Also for higher frequencies the coherence is bad. Apparently a linear model is a good approximation for H_1, but not for H_2. Although these results aren't very good, they are the only ones available so they will have to be used.

In order to derive a model that is suited for computer implementation these transfer functions are fitted with a 4th order model by the help of the program in Appendix B. In Figures 4.2 and 4.3 the fitted and the measured transfer functions are plotted. These fitted

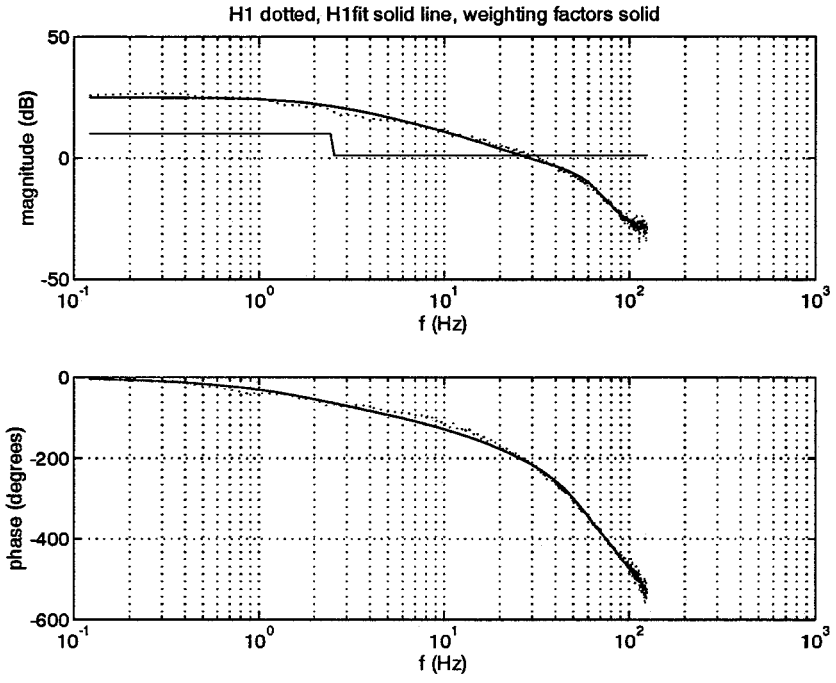

Figure 4.2: The transfer function H_1 and its fit

transfer functions are still not suited for simulations, because the real transfer functions H_1 and H_2 descend to zero for frequencies beyond the plotted range. The fitted ones remain at a certain constant value for high frequencies and therefore a low pass filter with $f_{cutoff} = 500$ Hz has been implemented.

Now we have a pressure model that can be used for simulations. In Figures 4.4 and 4.5 the real step responses of the CVT and the step responses simulated with the fitted transfer functions are given. We see that the real CVT response depends on several aspects that weren't taken into account when developing the pressure model, like for example the CVT ratio (that varies during the measurements of the step response) and the oil temperature. We can also see that, in a qualitative way, the real and the simulated step responses resemble each other pretty much. Thus we state that the model is suited for testing the control laws. By adding noise at several places in the simulation model an attempt is made to take into account the influences of some unmodelled factors. In this way it can be tested whether the control algorithm is able to maintain a good performance under changing operating conditions.

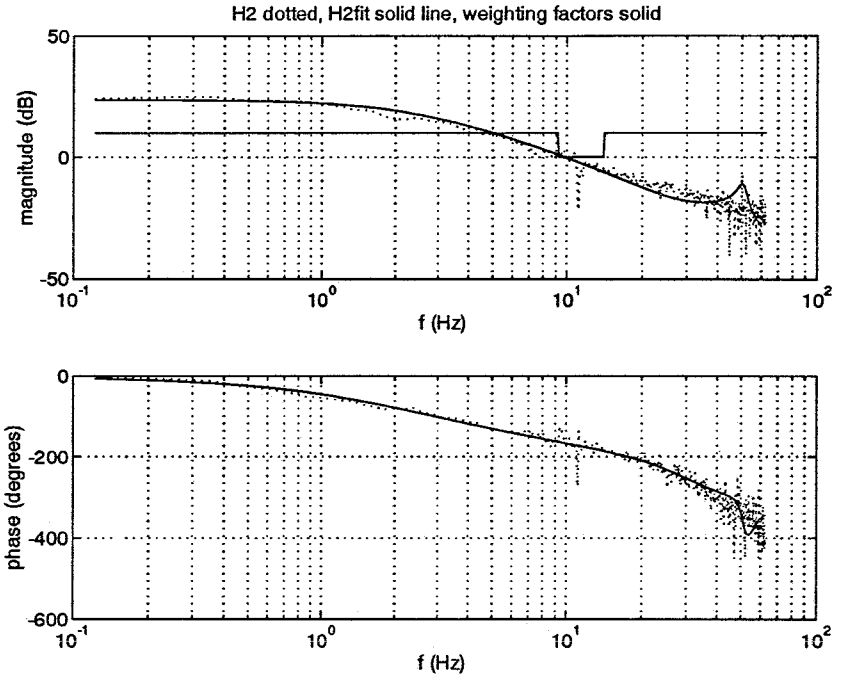

Figure 4.3: The transfer function H_2 and its fit

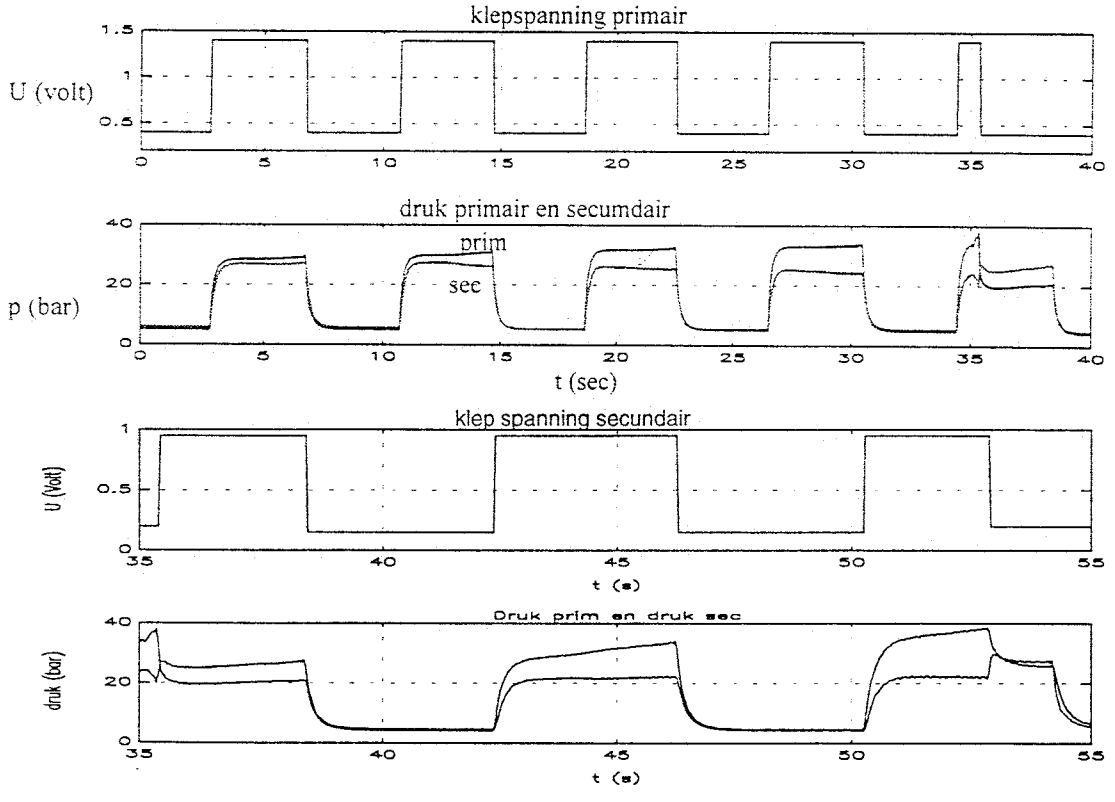

Figure 4.4: The step responses of the CVT

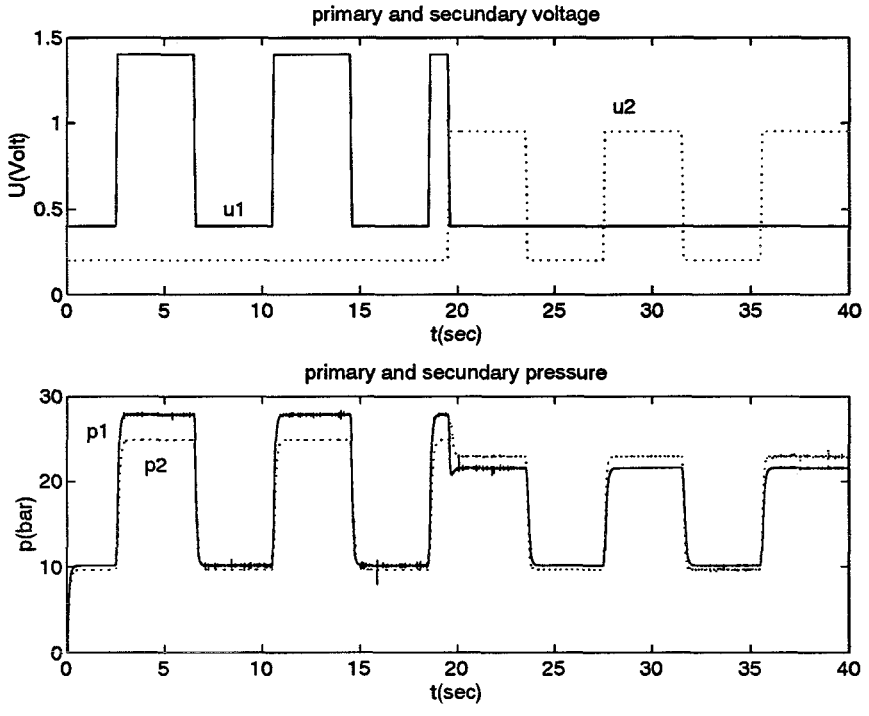

Figure 4.5: The simulated step responses with the pressure model

4.2 Simulating the whole CVT behaviour in SIMULINK

With this pressure model a simulation model for the whole CVT can be composed. The simulations have been performed in SIMULINK. In Appendix A the block schemes for SIMULINK are given. There are three main blocks: *CVT model*, *pressure control* and *rate of ratio change control.*

4.2.1 The CVT model block

This block represents the *pressure model* and the *flow model*. The *pressure model* block gives us the pressures p_1 and p_2 resulting from inputs u_1 and u_2. In the simulation model one way valves have been used. That's why these inputs have to be bounded, because for a voltage of zero these valves are completely closed, so negative inputs have no relevancy. In the pressure model we find the fitted transfer functions and the low pass filter. Because these functions aren't very accurate and also to simulate the dependency of the CVT behaviour on the ratio and the oil temperatures, noise has been added to both outputs p_1 and p_2. This noise has been determined previously and was saved in the files **p1ruis.mat** and **p2ruis.mat**. As can be seen in Appendix C these noise signals consist of a low frequency part representing changing oil temperatures and operating conditions and a high frequency part representing measurement noise. In Figure 4.6 the signals p_1 and p_2 - during a simulation - with and without added noise are plotted.

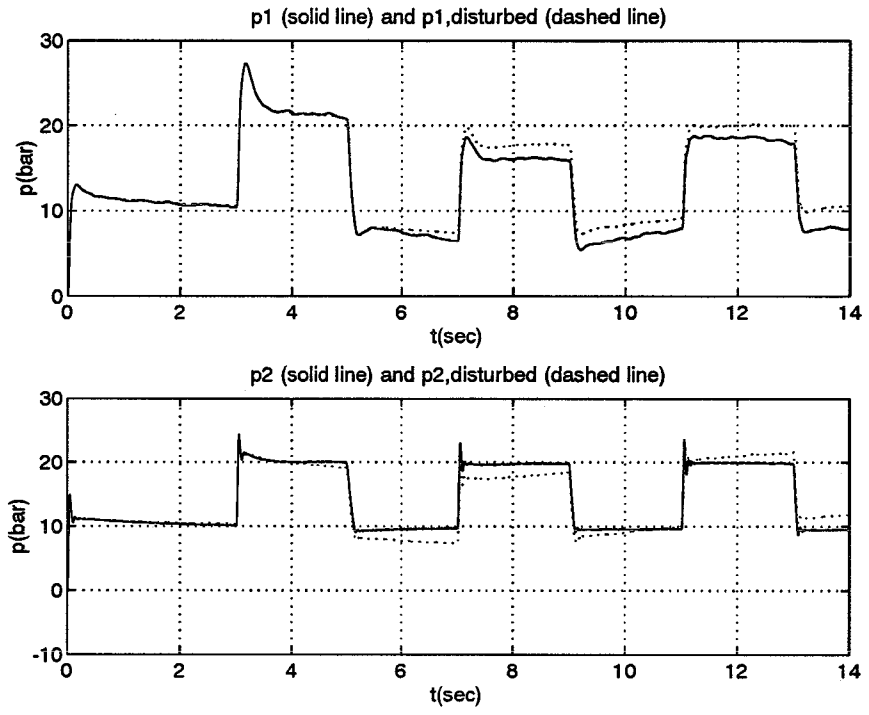

Figure 4.6: The original pressure signals and the disturbed ones

Another component of the *CVT model* is the *flow model*. In this block the oil flow Q_1 to the first pulley sheave is determined by means of the valve characteristic. In the manual of the valves this characteristic is given with a limited accuracy and especially for small flows, which appear very much in this application, the accuracy isn't very high. That's why noise - determined previously and saved in p2ruis.mat - has been added to the valve characteristic as well. As can be seen in Appendix C these noise signals also consist of a low frequency part representing the limited accuracy of the valve characteristic and changing oil temperatures and a high frequency part representing measurement noise of the signal $\frac{di}{dt}$. In Figure 4.7 the valve characteristics with and without added noise have been plotted. Now with relation 2.1 we can find the rate of ratio change ρ and by integrating this the ratio i. A low pass filter has been implemented in order to model the combined compliance of the hydraulic fluid and the oil chamber.

4.2.2 The pressure control and rate of ratio change control blocks

In these blocks the control signals are determined. The *pressure control* block is split up in three other blocks: *reference pressure model*, *calculation adaptation parameters*, *calculation u2*. The *rate of ratio change control* block makes use of one other block that calculates the value of the adaptation parameter *dq*, where this block (*calculation dq*) uses the block *reference ratio model*.

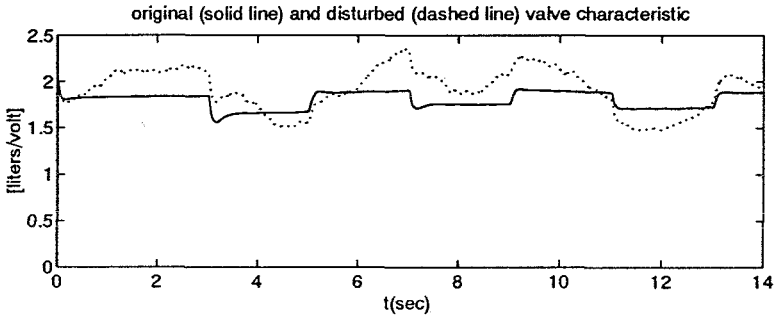

Figure 4.7: Original and disturbed valve characteristic

4.3 Experiments

In Appendix D the values for the variables in the control law are given. Experiments have been performed with three different control configurations:

1. The control law developed by E. Spijker without interaction between the pulley chambers, so $\alpha = 0$. For the variables in the *calculation adaptation parameters* block the following values were chosen: $\kappa_1 = -0.8 \cdot 10^{-3}, \kappa_2 = 0.8 \cdot 10^{-3}, \kappa_3 = 0$.

2. A control law with interaction between the pulley chambers. In this case the optimal value for α appears to be 0.45. For the variables in the *calculation adaptation parameters* block the following values were chosen: $\kappa_1 = -0.8 \cdot 10^{-3}, \kappa_2 = 0.8 \cdot 10^{-3}, \kappa_3 = -0.2 \cdot 10^{-3}$.

3. A control law with interaction between the pulley chambers, while the value of α is adapted on line by the adaptive control system. The variables in the *calculation adaptation parameters* block are: $\kappa_1 = -0.3 \cdot 10^{-3}, \kappa_2 = 0.3 \cdot 10^{-3}, \kappa_3 = -0.5 \cdot 10^{-5}$.

In the experiments the step responses of the CVT with the three different control configurations have been tested. In this situation a step of $p_{s,set}$ is performed simultaneously with a step of ρ_{set}. This is a practical situation because a higher value of ρ results in a higher torque and thus a higher value of p_s. Though in the experiments the value of $p_{s,set}$ remains constant for a certain constant value of ρ_{set} (so varying value of i), which isn't corresponding with Eq.2.2, these signals are suited very well for testing the controller performance.

4.4 Results

Figure 4.8 shows that there are no differences between the three controller configurations, concerning the control of $\frac{di}{dt}$. They all realize good tracking, while the effects of the noise on the valve characteristic are still visible. By choosing a faster adaptation speed for d_q or higher values for k_q and m_q these effects can be made smaller but that results in a higher overshoot and more oscillations when a step in $\frac{di}{dt}$ is made.

In Figure 4.9 a comparison is made between the pressure responses of configuration 1 and configuration 2. The performance of configuration 2 is better, i.e. the response is as fast but the overshoot is reduced with a factor two. Both controllers succeed pretty well in reducing the influence of the noise added to the system. This figure also shows that the response for

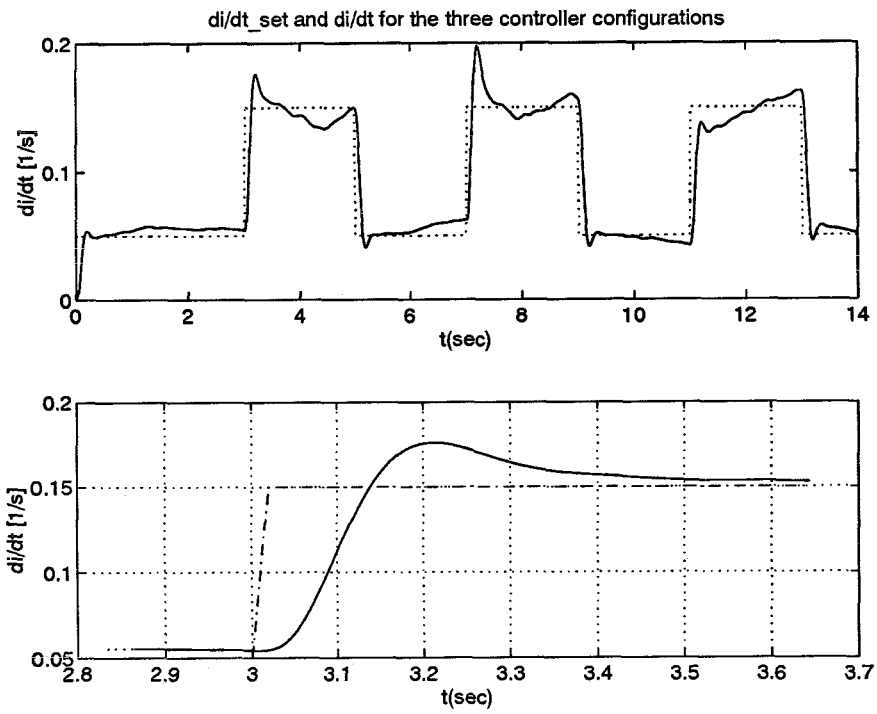

Figure 4.8: The rate of ratio controller performances

an increasing pressure signal is much faster than for a decreasing pressure. This is caused by the fact that in the simulation model one way valves have been used. That's why the oil flow through the valve can only go into the pulley chamber, so a decreasing pressure can only be caused by oil leakage, not by an oil flow through the valve. In the simulation model this corresponds with the positively bounded values of the input signal u_p and u_s. This response can also be made less sensible for disturbances (noise added to the system) by choosing higher adaptation speeds for k_r and m_r but this results in a higher overshoot and more oscillations.

Figure 4.10 shows that there is hardly any difference between the performances of configurations 2 and 3, where the remark should be made that only a low adaptation speed was chosen for α, because a higher speed resulted in more oscillations. That's why also the adaptation speeds of k_r and m_r were set to lower values. During these simulations the value of α varied around its initial value of 0.45.

It should be remarked that the performance depends very much on the value of the controller parameters. It is possible to obtain about the same effect by varying one parameter as by varying another. For example increasing the adaptation speed of pressure controller parameters k_r and c_r results in more oscillations and better disturbances rejection. So does increasing the adaptation speed of α, the degree of interaction. This makes it difficult to find the optimal values for the controller parameters.

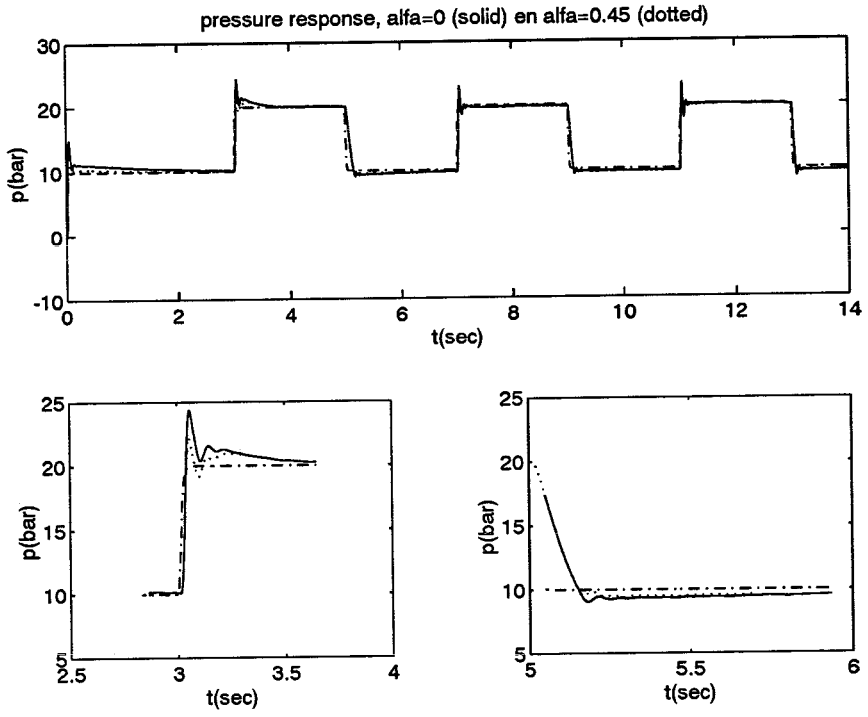

Figure 4.9: The pressure response controller performances

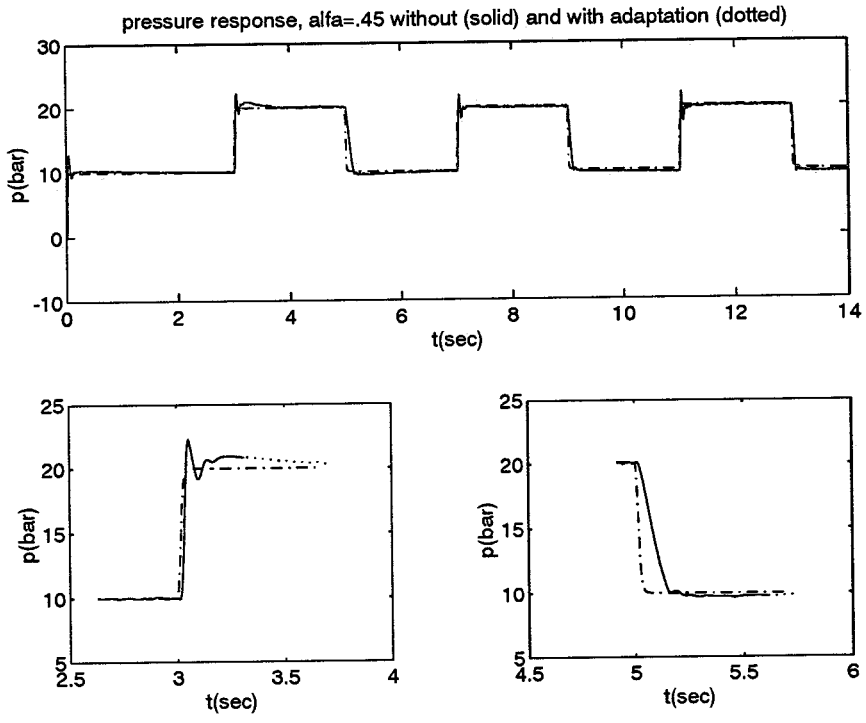

Figure 4.10: The pressure response controller performances

Chapter 5

Conclusions and recommendations

5.1 Conclusions

The controller that takes into account the interaction between the pulley chambers realizes a better pressure response. Little improvement is attained by adapting the degree of interaction (α) on-line. Regarding the rate of ratio change response no gain is to be seen. Because the rate of ratio response is the most critical, the improvement with respect to the existing controller is marginal.

The fact that the rate of ratio change performance didn't improve is caused by the fact that the flow into the primary pulley chamber is determined by the valve characteristic. In that valve characteristic only the value of p_p is important, while that value is measured every time a new input signal has to be calculated. So taking into account the influence of pressure p_s on p_p doesn't substantially improve the performance, though one should think the reduction of the oscillations of p_p, attained by the improved pressure control law, would result in less oscillations of the rate of ratio also.

The controller performance hasn't been tested for time-varying input signals. These signals might cause some problems, because the use of the reference models in the control law design doesn't assure correct following of these signals.

The problems concerning the value of $\dot{p}_p$, which were expected, didn't show up in the simulations. This is probably caused by the fact that the measurement noise in the computer simulations is not as high as in practise.

5.2 Recommendations

In order to improve the rate of ratio change performance it will probably be necessary to follow another control strategy. It's impossible to improve the performance of this flow control system by taking into account the interaction between the pulley chambers. That only improves the pressure response, not the rate of ratio response as stated in the previous section.

The pressure controller might be further improved by making the degree of interaction α frequency dependent in a way corresponding with Fig. 2.3 or by not making the simplification that $H_2 = \alpha H_1$. This would result in a more complicated controller of higher order.

The controller performance can be improved by using two-way valves like in the real CVT, instead of the one-way valves which are implemented in the computer model. This would especially improve the performance for a step from a higher to lower value.

The problems concerning the value of $\dot{p}_p$, which will probably arise when this control law would be implemented in practise could probably be solved by developing another control law. The strategy to be followed would be the following: u_p in Eq.3.2 shouldn't be substituted by Eq.3.3. For the further derivation of the control law equation Eq.3.2 should be used instead of Eq.3.4. Now $\dot{p}_p$ isn't necessary any more, while the value of u_p in Eq.3.2 is always known because it is calculated in the rate of ratio control law.

Appendix A

Simulink block schemes

Main scheme

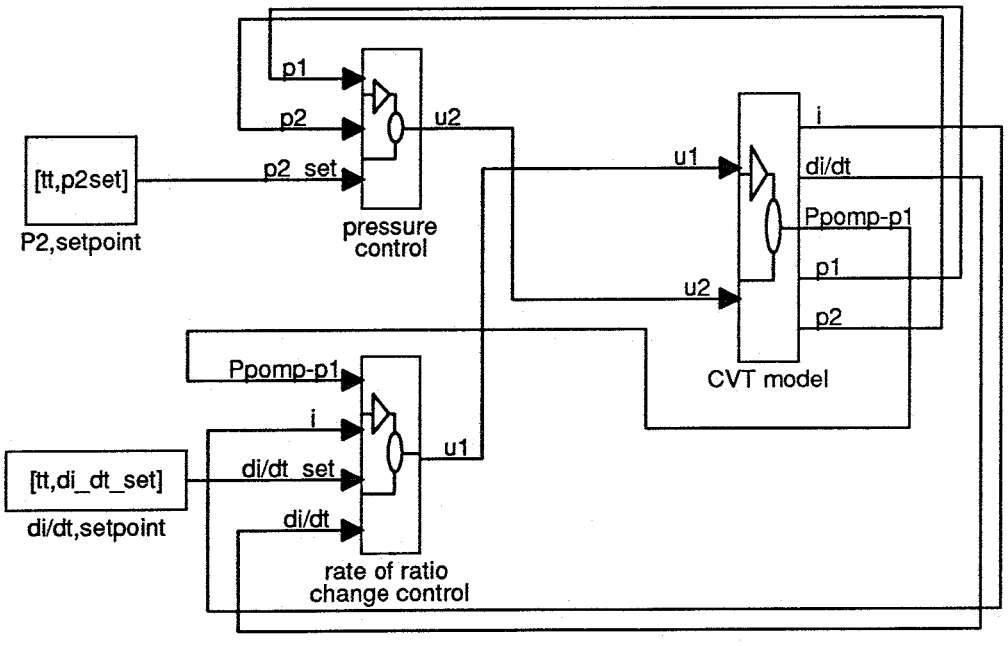

CVT model

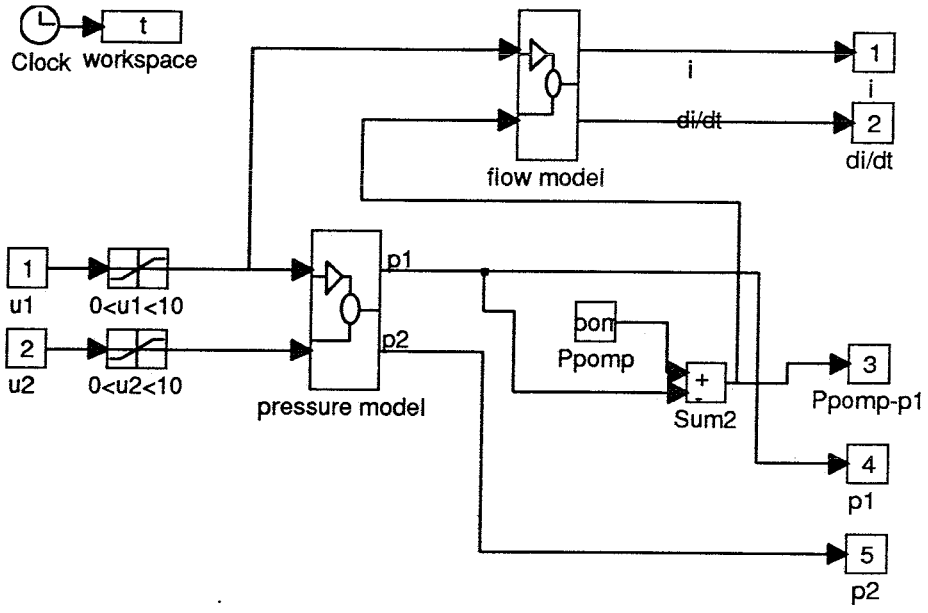

pressure model

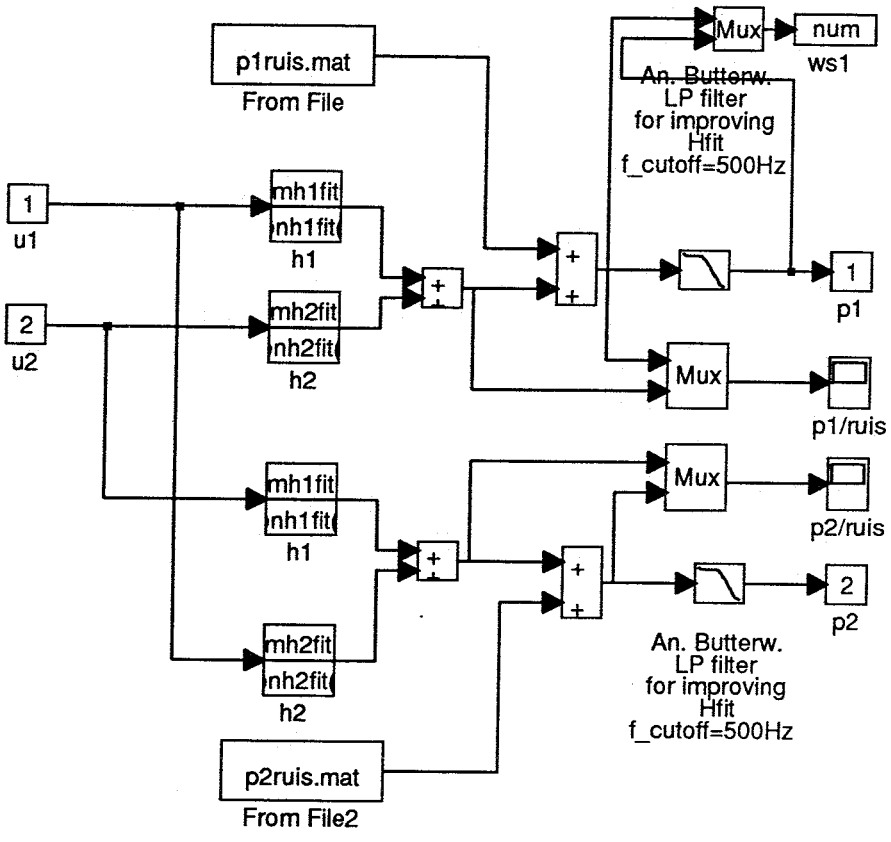

flow model

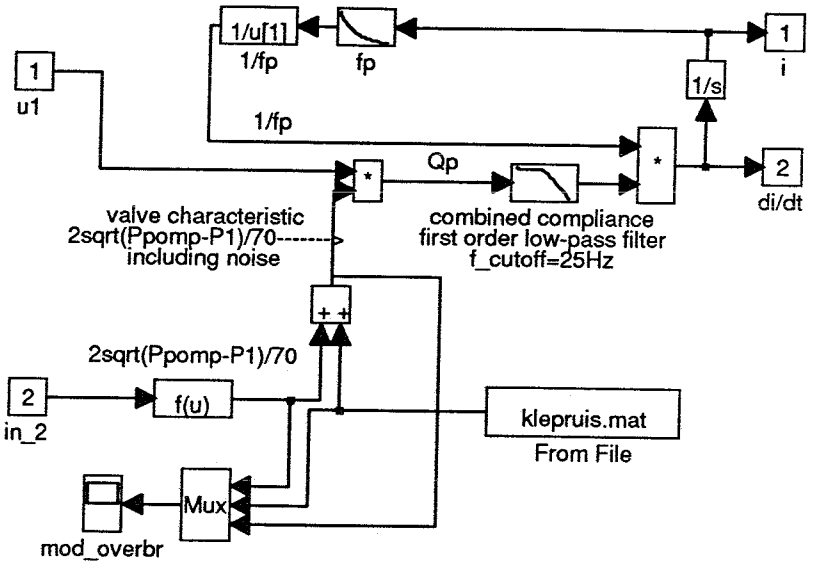

pressure control

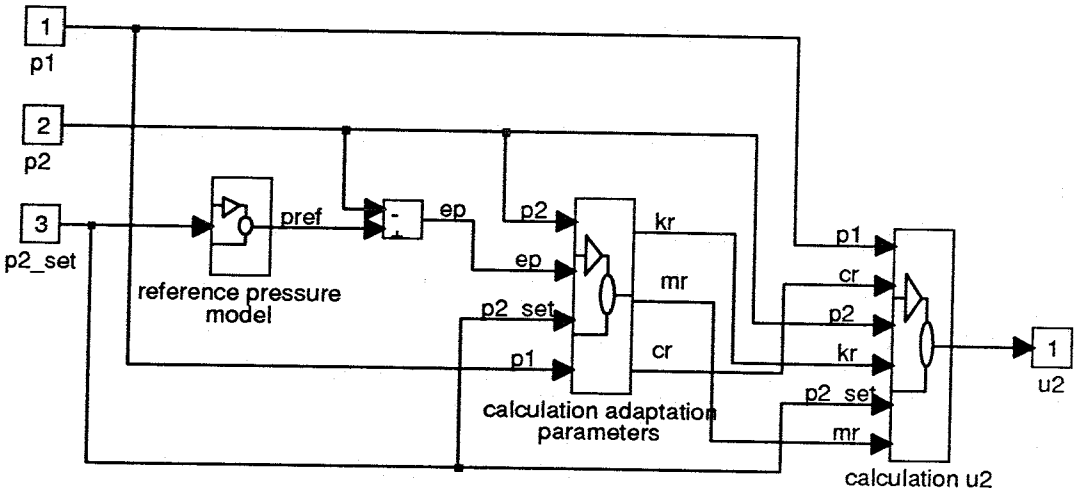

reference pressure model

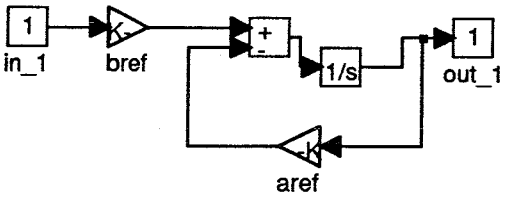

calculation adaptation parameters

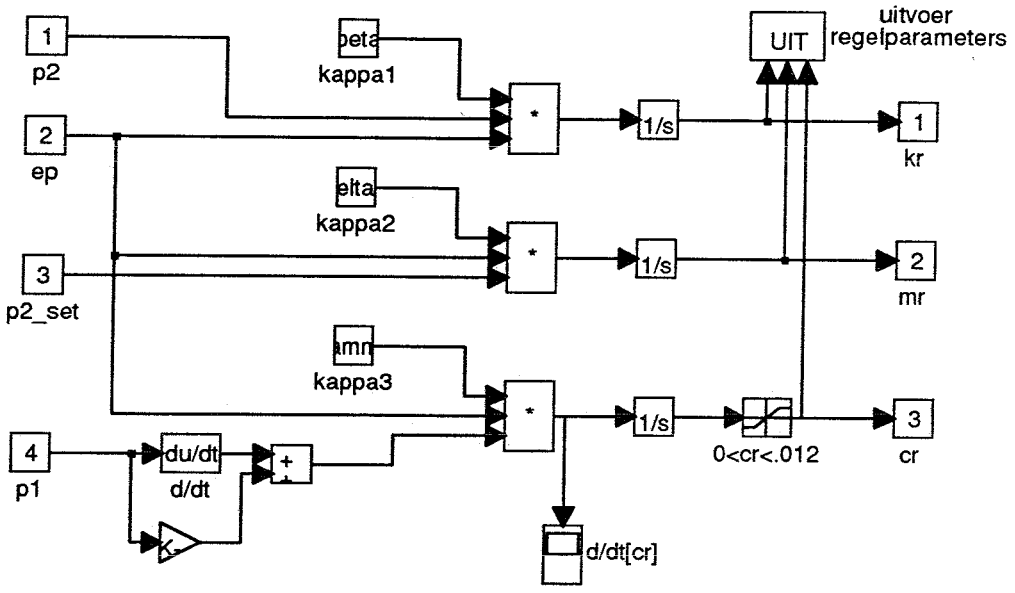

calculation u2

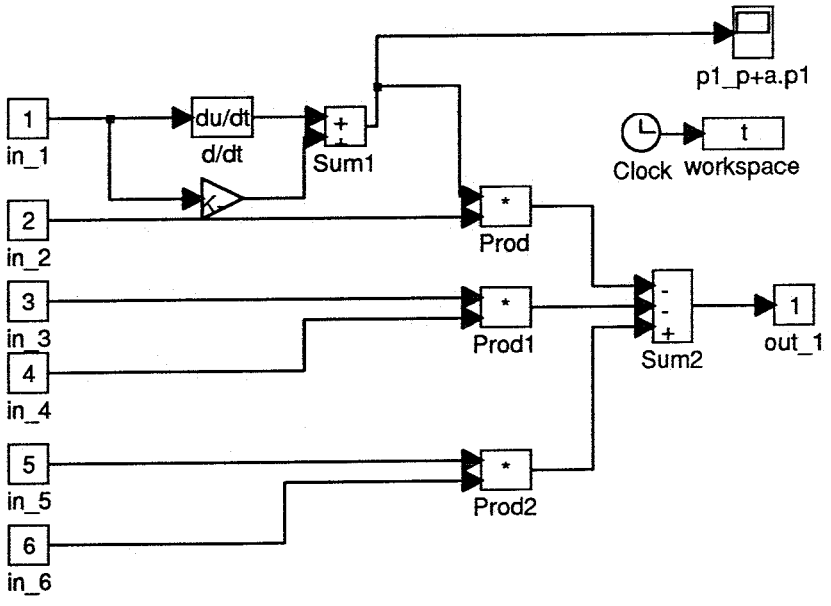

rate of ratio change control

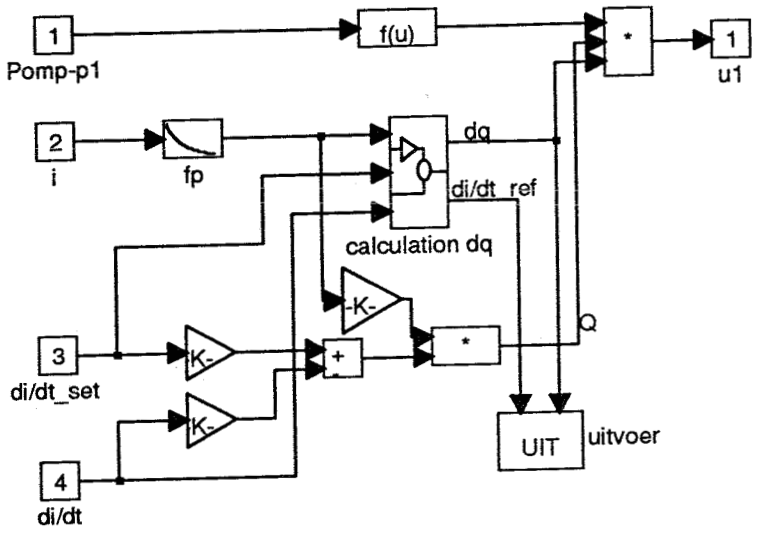

calculation dq

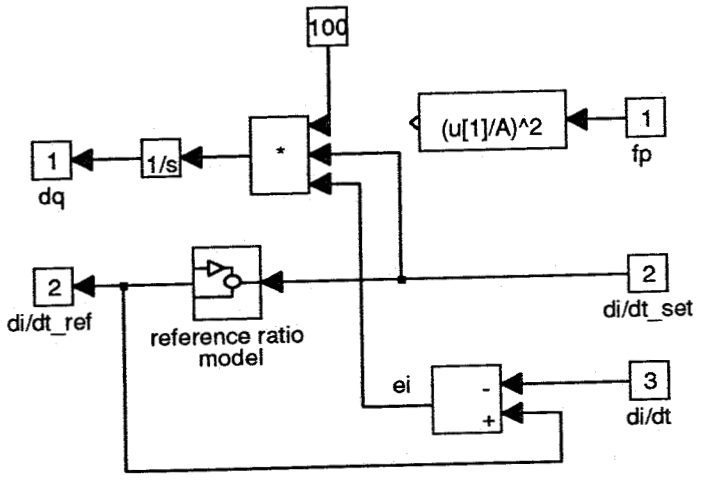

reference rate of ratio model

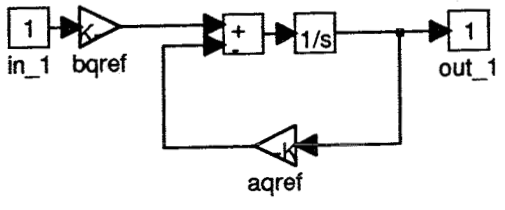

Appendix B

Matlab program for fitting transferfunctions

simulh.m

```
clear
load h1h2
h1=P1up(:,4);
h2=P1us(:,4);
weeg1=[10*ones(1,20) ones(1,1004)];
[numh1fit,denh1fit]=invfreqs(h1,2*pi*f,4,4,weeg1)      % fitten H1
[magh1fit,phaseh1fit]=bode(numh1fit,denh1fit,2*pi*f);

axis([-1 2 -20 40]);
clg
subplot(211);
semilogx(f,20*log10(abs(P1up(:,4))),'k:',f,20*log10(magh1fit),'k',f,weeg1,'k');
title('H1 dotted, H1fit solid line, weighting factors solid')
grid
xlabel('f (Hz)');ylabel('magnitude (dB)');

subplot(212);
axis([-1 2 -400 0])
semilogx(f,unwrap(angle(P1up(:,4)))/pi*180,'k:',f,phaseh1fit,'k');
xlabel('f (Hz)');ylabel('phase (degrees)');grid

pause

weeg2=[ones(1,75) .00001*ones(1,40) ones(1,105) ones(1,292) zeros(1,512)];
[numh2fit,denh2fit]=invfreqs(h2,2*pi*f,4,4,weeg2)      % fitten H2
[magh2fit,phaseh2fit]=bode(numh2fit,denh2fit,2*pi*f);

clg
axis([-1 2 -60 40]);
subplot(211);
```

```
semilogx(f(1:512),20*log10(abs(h2(1:512))),'k:',
        f(1:512),20*log10(magh2fit(1:512)),'k',f(1:512),10*weeg2(1:512),'k');
title('H2 dotted, H2fit solid line, weighting factors solid')
grid
xlabel('f (Hz)');ylabel('magnitude (dB)');

subplot(212);
axis([-1 2 -400 0])
semilogx(f(1:512),unwrap(angle(h2(1:512)))/pi*180,'k:',
        f(1:512),phaseh2fit(1:512),'k');
xlabel('f (Hz)');ylabel('phase (degrees)');grid
```

Appendix C

Simulink block scheme for generating noise signals

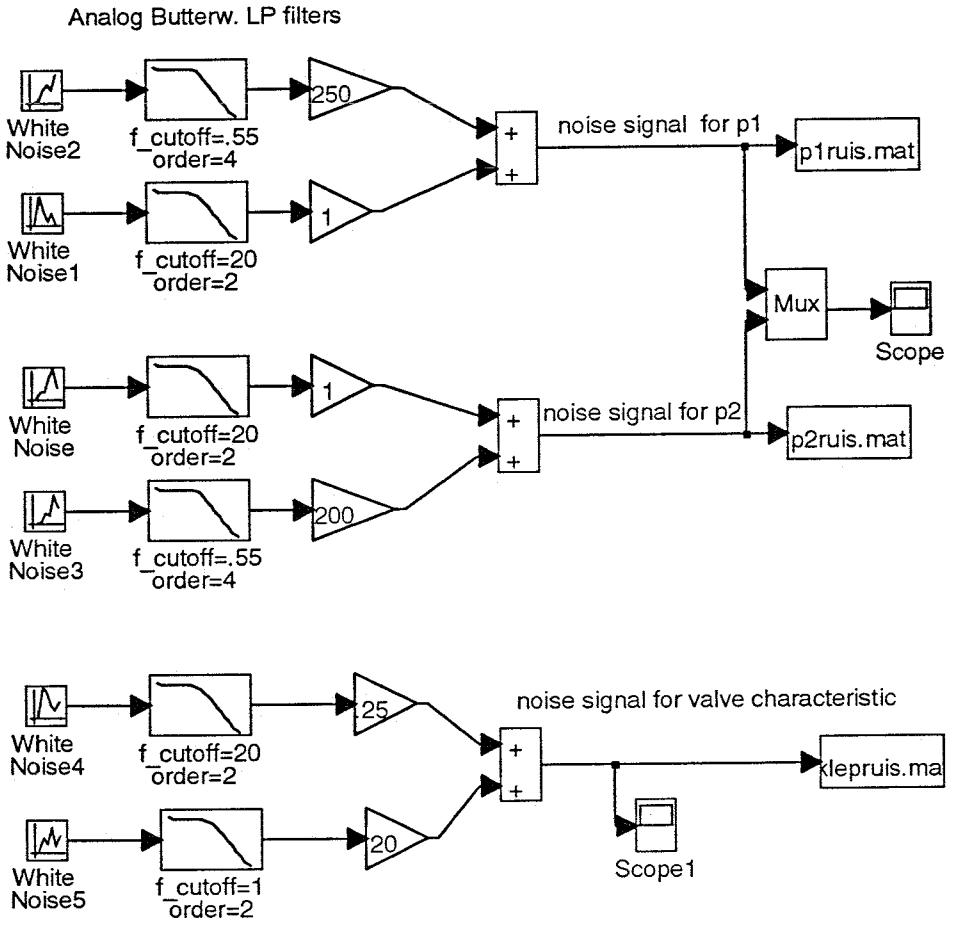

Appendix D

Initialisation of all variables

init.m

```
%  Initialisatie van variabelen

clear

% inlezen van de gefitte overdrachtsfuncties, bepaald via simulh

load hfit

% inlezen van functie f voor vollumestromen, bepaald via funcf

load func_f

% declareren van enkele variabelen

A=1;
Ppomp=70;
aref=2*pi*20;
bref=aref;
a=1.5*2*pi;
b=a*20;
aqref=20*pi*2.5;
bqref=aqref;
aq=2*pi*25;      % 25 Hz is de cutoff freq. van het filter in het flow model
bq=aq/A;
kq=(aqref-aq)/bq;
mq=bqref/bq;

beta=1;
delta=1;
gamma=2.7e-5;
alfa=0.45;
```

```
% genereren van de stapfuncties voor p2 en di/dt

tt=[.02:.02:14]';
di_dt_set=[.05*ones(1,150) .15*ones(1,100) .05*ones(1,100) .15*ones(1,100)
           .05*ones(1,100) .15*ones(1,100) .05*ones(1,50)]';
% di_dt_set=[di_dt_set(81:700,1) ;zeros(80,1)];  % opregelen di/dt niet gelijk
                                                 % met drukverhoging
                                                 % (niet in verslag)
p2set=[10*ones(1,150) 20*ones(1,100) 10*ones(1,100) 20*ones(1,100)
       10*ones(1,100) 20*ones(1,100) 10*ones(1,50)]';

% sinusvormige signalen (niet in verslag)
% di_dt_set=.1+.05*sin(tt);
% p2set=15+5*sin(tt);
```

References

- Spijker, E. 'Steering and control of a CVT based hybrid transmission for a passenger car', Master's thesis, Laboratory for Automotive Engineering, Eindhoven University of Technology, ISBN 90-386-0173-5, 1994.
- Spijker, E. 'An electronically controlled CVT for a flywheel-hybrid vehicle: Design development and validation of control algorithms', Laboratory for Automotive Engineering, Eindhoven University of Technology, Report no. WOC/VT/R/93.150, 1993.